

Characterisation of MgO-ZrO_2 precursor powders prepared by in-situ peptisation of coprecipitated oxalate gel

T. Settu*

Dalmia Institute of Scientific and Industrial Research, Opp. Arabic College, Vellakkalpatty, Salem-636 012, India

Received 30 June 1999; received in revised form 26 August 1999; accepted 21 September 1999

Abstract

Chemical precipitation–peptisation is adapted to produce fine powder of MgO-ZrO_2 using metal salts of chloride, nitrate and oxalic acid in triple distilled water. Co-precipitated magnesium–zirconyl oxalate gel is oven dried and the powder is used to prepare sol and subsequently gel. Both the precipitated and the sol–gel powders are calcined at different temperatures for 1 h and are subjected to powder X-ray diffraction to ascertain the crystalline nature. TGA and DTA analysis is carried out to study the thermal decomposition and phase transition behaviour. Surface area of the powders, calcined at different temperatures, is also determined using BET technique. Effect of alcohol washing on the precipitated powder is also reported. © 2000 Elsevier Science Ltd and Techna S.r.l. All rights reserved.

Keywords: MgO-ZrO_2 powders; Coprecipitation; Oxalate gel

1. Introduction

Primary requirements for high-performance engineering ceramic materials are high density and homogeneous microstructure with optimum grain size. In order to achieve these goals, processed powders should possess necessary morphology, sinteractivity and purity. Particularly for zirconia ceramic material, the processing parameters should be controlled to stabilise high temperature phases, tetragonal and cubic, to ambient condition, to utilise its potential applications. The phases are stabilised by making solid solutions with number of additives such as CaO , MgO , CeO_2 , Y_2O_3 and with other rare earth oxides.

In order to have homogeneous mixing of additives with parent material, non-conventional methods of preparation yield optimum results. There are many routes available for preparation of zirconia/stabilised zirconia ceramic fine powders like alkoxide decomposition [1,2], controlled hydrolysis to obtain monosized powder [3,4], hydrolysis of inorganic salts and alkoxides [5–7], transparent monolithic gel [8], chloride precipitation [9–11], oxalate physical gelation [12–14], soft agglomerated powders by alcohol washing [11,15], etc.

Readey et al. [11] and Kaliszewski and Heuer [15] have suggested that alcohol washing of precipitated gel yields soft agglomerates. They have pointed out that ethanol washing of precipitated hydroxide gels leads to formation of surface ethoxy groups which inhibits formation of direct bonding, during drying, between inter particles thereby producing soft agglomerates.

Purpose of the present work is to prepare and characterise three different powders (co-precipitated, peptised sol–gel and alcohol–ethanol washed powders) of 7 mol% of magnesia stabilised zirconia by chemical precipitation–peptisation method. First the metal ions are coprecipitated using oxalic acid solution and then metal oxalate sol is prepared by means of in-situ peptisation. The dried gel powders are characterised by powder X-ray diffraction, TGA, DTA and determination of surface area using BET technique.

2. Experimental procedure

2.1. Coprecipitation of MgO-ZrO_2

Powder samples used in this work were prepared by the method reported elsewhere [13] with modification. $\text{ZrOCl}_2 \cdot 8\text{H}_2\text{O}$ (LR Grade, CDH Chemicals, India),

* Tel.: +91-427-447412; fax: +91-427-331098.

E-mail address: tsettu@hotmail.com (T. Settu).

$\text{Mg}(\text{NO}_3)_2 \cdot 6\text{H}_2\text{O}$ (AR Grade, CDH Chemicals, India), $(\text{HCO}_2)_2 \cdot 2\text{H}_2\text{O}$ (AR Grade, SD Fine Chemicals, India) were chosen as starting materials because of their high solubility in water. Triple distilled water was used throughout the experiment as solvent. Solutions of 0.7 M of $\text{ZrOCl}_2 \cdot 8\text{H}_2\text{O}$, $\text{Mg}(\text{NO}_3)_2 \cdot 6\text{H}_2\text{O}$ (corresponding to 7 mol% of MgO and 93 mol% of ZrO_2 in the final oxide powder) and $\text{H}_2\text{C}_2\text{O}_4 \cdot 2\text{H}_2\text{O}$ were prepared by slowly adding the respective salts in a constantly stirred water containing glass beaker.

The prepared solutions of $\text{ZrOCl}_2 \cdot 8\text{H}_2\text{O}$ and $\text{Mg}(\text{NO}_3)_2 \cdot 6\text{H}_2\text{O}$ were intimately mixed in a glass beaker using a stirrer and paddle. Then, the $\text{H}_2\text{C}_2\text{O}_4 \cdot 2\text{H}_2\text{O}$ solution was added dropwise into the vigorously stirred mixed cation solutions, which yielded a white gelatinous precipitate and was allowed for 12 h to settle down. The resultant precipitate was filtered and divided into three batches, which were designated as P1, P2 and P3, respectively. The third batch of the precipitate was washed thoroughly with ethyl alcohol. All these powders were oven dried at 50°C until water gets evaporated.

2.2. In-situ peptisation of MgO–ZrO₂ precipitate

The dried friable gel, P2 was crushed to powder using a mortar and pestle. The powder was again, kept in a hot air oven at 100°C for 15 min. The dried powder was then gently added into stirred water contained in a glass beaker (quantity of water was same as used for preparation of 0.7 M solution). The stirring was continued until a very clear sol was formed. The resultant sol was kept as such for gelation. The clear gel was again oven dried at 50°C and was crushed to powder using a mortar and pestle.

The dried powders P1, P2 and P3 were all calcined at 470, 600 and 850°C for 1 h to ascertain crystallisation temperature using powder X-ray diffraction. In order to analyse the thermal decomposition and phase formation behaviour, TGA and DTA spectra were recorded. Specific surface area was determined by BET technique using nitrogen gas as adsorbent.

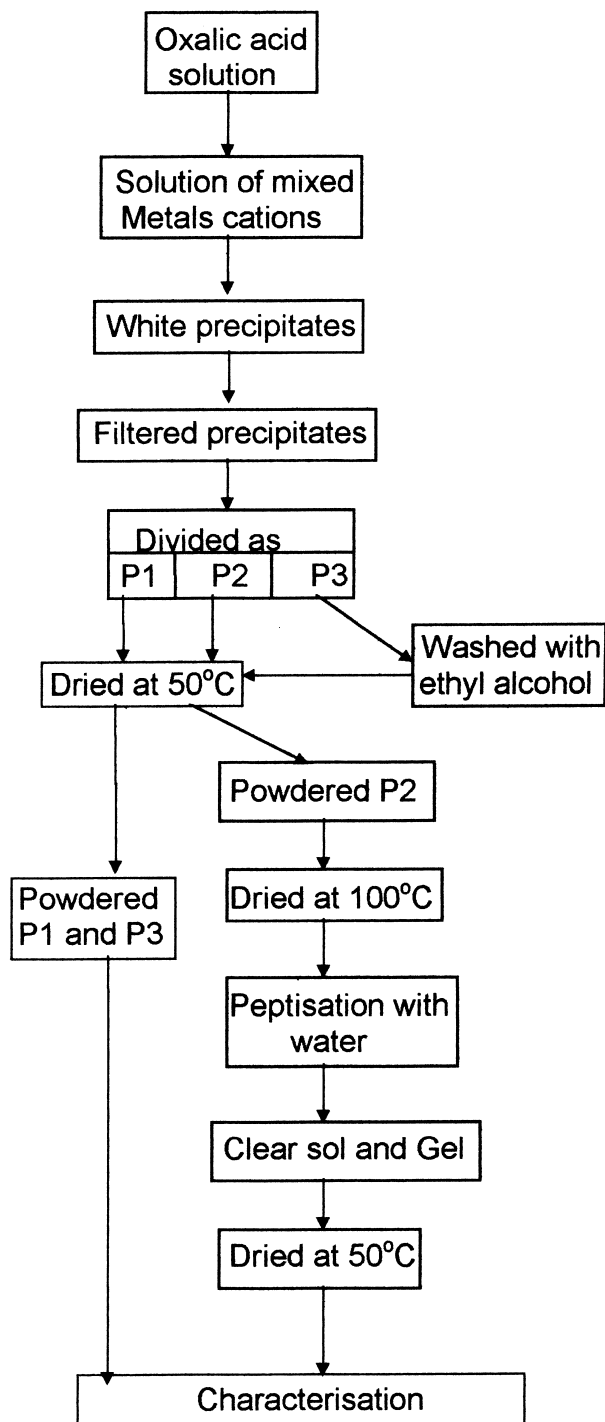
Scheme 1 shows the experimental procedure for the preparation of these powders.

3. Results and discussions

3.1. Preparation of oxalate precipitates and sol

The oxalic acid solution is gently added in a glass beaker, with stirring, which contains combined cation solution. Immediately after the addition of oxalic acid, white precipitates were formed and disappeared automatically. The formation of white precipitates may be due to localised super saturation of ions in the solution. Further continuation of stirring leads to homogenisation

of ions in the solution, which favours the disappearance of the precipitates. If the addition of oxalic acid continues, the rate of disappearance of the precipitates decreases which may be due to the increase of ionic concentration. This enables super saturation of the solution and hence nucleation starts which leads to formation of aggregates and finally, a stable white fine precipitate is formed. This may be the reason for the



Scheme 1. Flow chart for preparation of different powders.

decrease in the rate of disappearance of the precipitates and for the formation of stable white precipitates.

The filtered dried precipitated powder is used to prepare the sol and subsequently gel. The dried powder P2, is gently added to water with continuous stirring. The powder slowly gets peptised and forms a clear sol which is an in-situ peptisation. Possible reason for the formation of sol is presence of residual hydrochloric acid, which is formed during the reaction of reactants, in the dried precipitated powder. While mixing of powder with water, the presence of HCl acid leads to peptisation of the oxalate powder and finally gives a clear sol. The existence of chloride ions are confirmed by using Volhard's volumetric method. The volumetric analysis shows that the chloride ion concentration is around 0.02 mols/l in the peptised sol. The clear sol is kept as such without any disturbance until it becomes a gel.

3.2. Crystallisation behaviour

Fig. 1 shows powder X-ray diffraction pattern for the as-dried samples of different powders. For the as precipitated dried powder P1, it is seen that it has fine crystalline nature. Amorphous character is observed

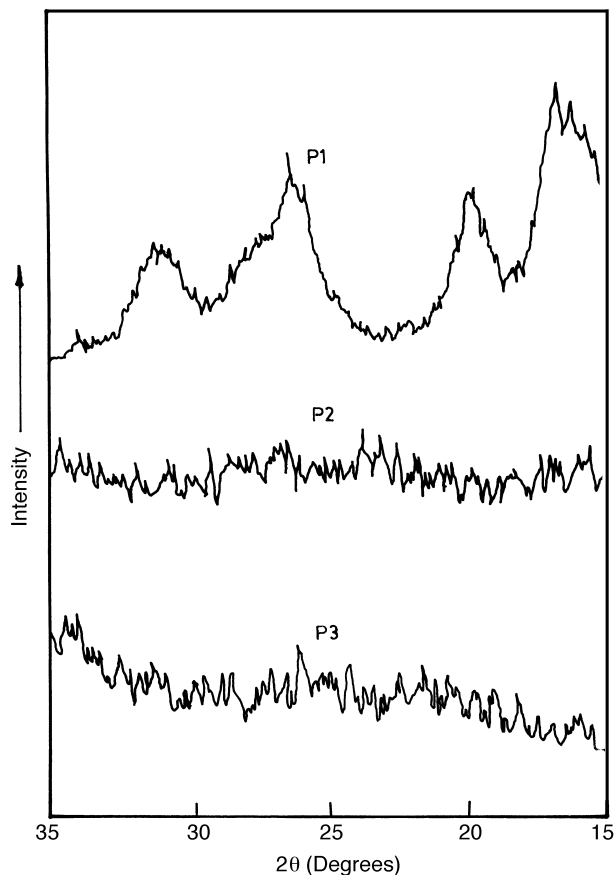


Fig. 1. X-ray diffraction pattern for the uncalcined powders: P1, as-precipitated powder; P2, peptised powder; P3, alcohol washed powder.

from XRD pattern for the peptised powder P2, and the alcohol washed powder P3.

Powder X-ray diffraction pattern for the isothermally heat treated samples at different temperatures is shown in Fig. 2. The dried powders start to crystallise at 470°C, in tetragonal phase for all the three samples and above this temperature, the crystalline nature increases with the *t* phase. (Diffraction pattern at 600 and 850°C are not shown in Fig. 2 for samples P2 and P3, which are same as powder P1.)

It can be observed from the powder X-ray diffraction results, the patterns for the as-dried powders are quite different in nature. The as-precipitated powder shows fine crystalline nature whereas the other two powders show the amorphous character. During washing of the powder P3 with alcohol, the tiny agglomerated oxalate crystals may be further dispersed in such a way that the powder is amorphous for the X-rays. The precipitated powder may form an amorphous network during

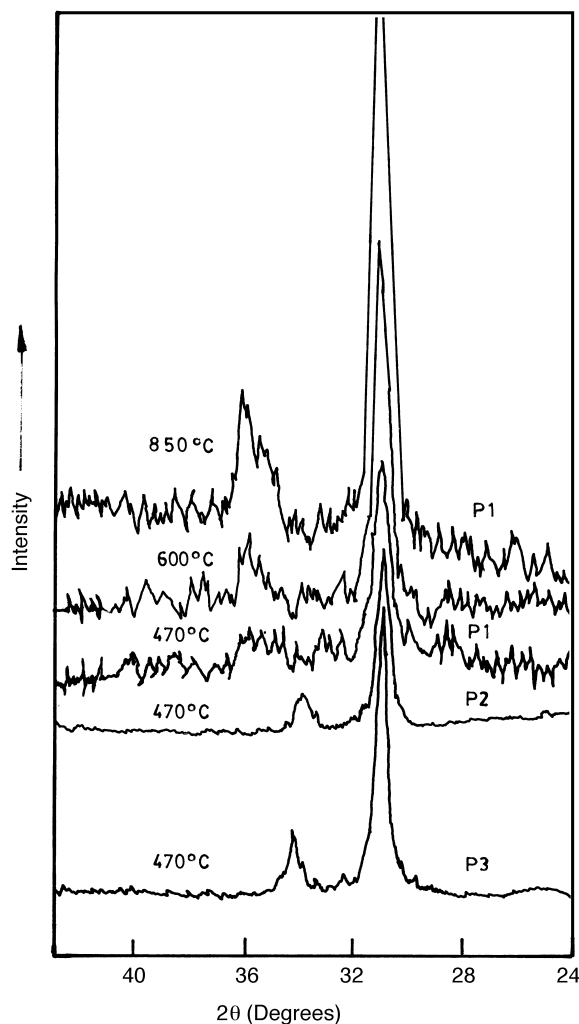


Fig. 2. X-ray diffraction pattern as a function of heat-treatment for the different samples: P1, as-precipitated powder; P2, peptised powder; P3, alcohol washed powder.

peptisation process so that it is also amorphous for the X-rays. Increase of crystallite size of calcined powders has been clearly reflected in the X-ray diffraction curve as width of the pattern decreases with increase of calcining temperature.

3.3. Thermal dependency studies

3.3.1. Thermogravimetry analysis

In order to study the thermal decomposition behaviour of dried powders TGA spectra were recorded in air atmosphere at a heating rate of $10^{\circ}\text{C}/\text{min}$, for all the three samples up to 850°C (for DTA studies also, the same condition was adopted). It is seen from the Fig. 3, for powder P1, there are two major steps of weight changes, 16.10 and 31.52% were observed in the temperature range 50 – 450°C . The first weight loss around 170°C is attributed to liberation of physi-sorbed water. Major weight loss around 340°C may be due to the decomposition of organics. Three more weight losses of 2.15, 1.68 and 2.88% have also been observed. The loss around 270°C may be due to the decomposition of nitrates and the last two weight changes around 470 and 590°C are probably, liberation of occluded/adsorbed chlorides and residual carbonates in the dried gel powder, respectively.

From the figure, TGA curve for the reprecipitated, dried gel powder, P2, it can be noticed that the weight losses and their corresponding stages, such as evaporation of water, decomposition of nitrates and oxalates, and adsorbed chlorides are almost same as those observed for the sample P1. Appreciable difference in weight loss for chloride liberation, is observed in the temperature range 450 – 525°C . Based on previous experiences [12,13], estimation of chloride ions by Volhard's volumetric method, has been carried out and is found that the existence of chloride ions in the reprecipitated dried gel powder, P2, is lower than the powder, P1.

It can be seen from Fig. 3, TGA curve for the ethyl alcohol washed, dried sample P3, that the weight loss

trend are almost same as the samples P1 and P2. Interestingly, the percentage of weight loss and the weight loss temperature are different. There are two weight losses of 9.25 and 55.67% that are observed in the temperature range 50 – 450°C . The loss around 145°C is due to the release of adsorbed water and the major loss around 350°C corresponds to decomposition of oxalate. The final weight losses of 1.12 and 1.58% may be due to the liberation of chlorides and residual carbons.

It is quite interesting to note from the three TGA curves namely, P1, P2 and P3, that there is a major difference in weight loss found only for the powder, P3. The weight losses of adsorbed water for P1 and P2 is more than P3 whereas in the case of organic decomposition for powder P3, is higher than the powders P1 and P2. This may be attributed that part of the adsorbed water molecules are replaced by ethyl alcohol while washing the precipitated powder as was reported by Readey et al. [11] and Kaliszewski and Heuer [15]. The nitrate decomposition is also overlapped with the organic decomposition step for the powder P3, where as, for the other powders, P1 and P2, it is well resolved.

3.3.2. Differential thermal analysis

Fig. 4 shows the DTA curve for the powder P1, P2 and P3 in the temperature range 100 – 800°C . It has been observed that there are two major endothermic peaks in the curve corresponding to liberation of adsorbed water around 170°C and oxalate decomposition around 340°C which are well agreed with the thermal decomposition processes. There is an exothermic peak occurring around 478°C which is due to crystallisation of tetragonal phase of Zirconia. There is a small shoulder around 270°C which may be due to decomposition of nitrates as observed in the TGA curve. From the DTA curve, for the reprecipitated dried gel powder, P2, it can be seen that the trend is same as observed for the sample P1 except that there are small variations in different thermal change processes.

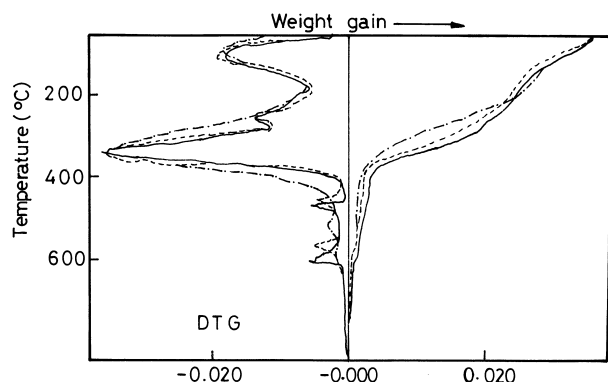


Fig. 3. TGA curves for different powders: —, P1; ---, P2; - · -, P3.

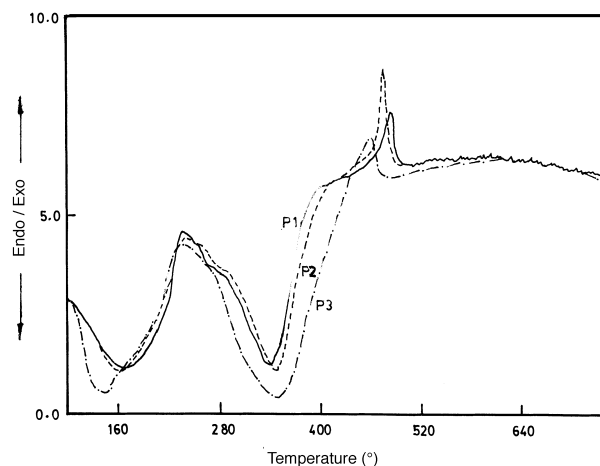


Fig. 4. DTA curves for different powders: —, P1; ---, P2; - · -, P3.

Table 1
Variation of surface area as a function of temperature measured by BET technique

	P1			P2			P3		
Calcination temperature (°C)	470	600	850	470	600	850	470	600	850
Specific surface area (m ² g ⁻¹)	48	22	6	55	28	8	68	37	11
Average crystallite size (nm)	27	58	192	25	49	165	22	37	159

It is observed from the DTA curve for the sample P3, liberation of adsorbed water and decomposition of oxalate took place around 135 and 355°C, respectively, which are endothermic peaks. The decomposition of nitrate is overlapped with the oxalate decomposition process that can be observed in the TGA curve also. Exothermic peak around 460°C is attributed to crystallisation of tetragonal phase of zirconia.

From the DTA curves of samples P1, P2 and P3, crystallisation of tetragonal phase occurs at different temperatures for different samples. i.e. 478°C for sample P1, 470°C for sample P2, and 460°C for sample P3. This may be due to difference in surface free energy of the powders. Crystallisation of tetragonal phase of samples P1, P2 and P3 has been confirmed by the X-ray diffractograms for the samples that have been isothermally heat treated at 470°C. In addition to this the two endothermic peaks of water evaporation and oxalate decomposition of sample P3 is quite different when compared to the samples P1 and P2 which is due to alcohol washing. This difference is also observed in the TGA curves.

3.4. Surface area analysis

Specific surface area has been estimated for the different types of powders using BET technique, with nitrogen. The dried gel powders are calcined at various temperatures such as 470, 600 and 850°C for 1 h. Average crystallite sizes of the powder were calculated by assuming that the prepared powders are spherical in shape. From Table 1, it is clear that the surface area of powders decreases as the calcination temperature increases, due to the increase of crystallite size.

Although the peptised powder P2, is completely amorphous for X-rays, the surface area is lower than the alcohol washed powder P3 which again reflects the interaction of alcohol with surface of inter particles.

4. Conclusions

Three different powders of MgO–ZrO₂ are prepared by using chemical co-precipitation, peptisation and alcohol washing methods. X-ray diffraction pattern for the calcined powders reveal that all have crystallised in tetragonal phase. The precipitated and peptised powders show almost same characteristics for TGA and DTA analysis where as the alcohol washed powder behaves differently. Surface area analysis shows the alcohol washed powder has more specific surface area than the other two powders which is due to the interaction of alcohol with inter particle surfaces of powder.

References

- [1] K.S. Mazdiyasi, C.T. Lynch, J.S. Smith, *J. Am. Ceram. Soc.* 50 (1967) 532.
- [2] M.J. Verkerk, B.J. Middelhuys, A. Burggraaf, *Solid State Ionics* 6 (1982) 159.
- [3] B. Fegley Jr, E. Barringer, in: C.J. Brinker (Ed.), *Better Ceramics Through Chemistry. Materials Research Society Symposia Proceedings*, Vol. 32. Elsevier, New York, 1984, p. 187.
- [4] K.S. Mazdiyasi, C.T. Lynch, J.S. Smith, *J. Am. Ceram. Soc.* 49 (1966) 286.
- [5] J. Livage, K. Doi, C. Mazieres, *J. Am. Ceram. Soc.* 51 (1968) 349.
- [6] N.H. Brett, M. Gonzalez, J. Bouillot, J. Niepce, *J. Mater. Sci.* 19 (1984) 1349.
- [7] Boro Duricic, Drago Kolar, Milos Komac, *J. Mater. Sci.* 25 (1990) 1132.
- [8] P. Kundu, D. Pal, Suchitra Sen, *J. Mater. Sci.* 23 (1988) 1539.
- [9] K. Haberk, A. Ciesla, A. Pron, *Ceramurgia Int.* 1 (1975) 111.
- [10] K. Haberk, *Ceramurgia Int.* 5 (1979) 148.
- [11] M.J. Readey, R.R. Lee, J.W. Halloran, A.H. Heuer, *J. Am. Ceram. Soc.* 73 (1990) 1499.
- [12] T. Settu, R. Gobinathan, *Bull. Chem. Soc. Japan* 67 (1994) 1999.
- [13] T. Settu, Ph.D. thesis, Anna University, Madras, India, 1995.
- [14] T. Settu, R. Gobinathan, *J. Eur. Ceram. Soc.* 16 (1996) 1309.
- [15] M.S. Kaliszewski, A.H. Heuer, *J. Am. Ceram. Soc.* 73 (1990) 1504.